Thermodynamics of Binding to SH3 Domains: The Energetic Impact of Polyproline II (P_{II}) Helix Formation[†]

Josephine C. Ferreon[‡] and Vincent J. Hilser*

Department of Human Biological Chemistry and Genetics, and Sealy Center for Structural Biology, University of Texas Medical Branch, Galveston, Texas 77555-1068

Received February 3, 2004; Revised Manuscript Received April 14, 2004

ABSTRACT: Although numerous biophysical studies have focused on elucidating the structural and thermodynamic determinants that govern the free energy of binding between various SH3 domains and their putative recognition sequences, a quantitative accounting of the energetics of this interaction has proven enigmatic. Specifically, the binding results in a large and negative change on the standard enthalpy and entropy functions, a result which is inconsistent with the positive values for these quantities that is expected from the hydrophobic nature of the binding pocket. Here, the binding of the C-terminal SH3 domain of Sem-5 to its putative recognition peptide on the Sos (Son of Sevenless) protein is investigated using isothermal titration calorimetry under a variety of temperature and pH conditions. In addition, the energy associated with folding the Sos peptide into the binding competent polyproline II conformation is quantitatively evaluated. These results provide a rationale for the observed discrepancy between the experimental and predicted behavior and indicate that the determinants of binding in this system cannot be ascertained from a static structural representation of the binding process.

Molecular recognition remains one of the most challenging problems in structural biology, and a complete understanding of this phenomenon can only come by elucidating the complex interplay between structure, dynamics, and energetics (*1*). SH3 domains play a crucial role in a variety of signal transduction pathways. These domains act by recognizing proline-rich sequences that adopt the polyproline II (P_{II}) conformation. Although numerous biophysical studies have focused on elucidating the structural and thermodynamic determinants that govern the free energy of the binding between SH3 domains and their putative recognition sequences (*2*, *3*−*7*), a quantitative accounting of the energetics of this interaction has proven enigmatic. Specifically, the binding interface between most SH3 domains and their peptide targets primarily consists of the hydrophobic surface area, the burial of which is expected to produce a net positive change in the standard enthalpy and entropy of binding (*5*). Nevertheless, high precision isothermal titration calorimetry (ITC)[1] studies on these SH3 domains (*2*, *5*, *6*, *8*−*10*) has revealed a net negative change on the standard enthalpy and entropy functions. The stark differences between the experimental and predicted behavior indicates that the thermodynamic determinants of binding do not rest exclusively in the contacts that are made in the interaction surfaces and that additional factors must be considered to quantitatively account for the energetics of binding.

Here, we use ITC to investigate the thermodynamics of binding between the C-terminal SH3 domain of the *Caenorhabditis elegans* protein Sem-5 (Figure 1) and the peptide corresponding to the recognition sequence of its binding partner, Sos (Son of Sevenless) (*11*), under different temperature, buffer, and pH conditions. In addition to experimentally measuring the thermodynamics of binding, we adopt a general partition function formalism that describes the energetics of redistributing the conformational ensemble of the peptide in response to binding. Using a surface-area based parametrization of the energetics, in conjunction with this ensemble description of the equilibrium, we derive quantitative estimates for the role of conformational redistribution of the peptide ensemble in determining the overall binding energetics. These results provide unprecedented insight into the energetic determinants of binding for SH3 domains and implicate redistribution of the peptide ensemble as being a major factor affecting the overall energetics of the interaction.

MATERIALS AND METHODS

Preparation of Sem-5 C-SH3 Domain. The cloning, expression, and purification of the C-terminal of the Sem-5 SH3 domain was as described previously (*12*). The Sem-5 C-SH3 used throughout the paper was the pseudo-wild type, wherein Cys209 was mutated to alanine to prevent possible oxidation and intermolecular cross-linking.

Preparation of Sos and SosY Peptides. The original Sos peptide has the sequence (Ac−PPPVPPRRR−NH_2). Because this sequence presents the problem of accurate peptide concentration determination, we adopted the peptide sequence used by Wittekind et al., (*10*, *13*) (Ac−VPPPVPPRRRY−NH_2) with an additional valine residue at the N terminus and tyrosine residue at the C terminus, which we define as the SosY peptide. The peptides were synthesized

[†] This work was supported by NIH Grant GM63747, NSF Grant MCB9875689, and Welch Foundation H-1461.

* To whom correspondence should be addressed. Fax: 409-747-6816. Tel: 409-747-6813. E-mail: vince@hbcg.utmb.edu.

[‡] Sealy Center for Structural Biology Pre-Doctoral Fellow.

[1] Abbreviations: SH3, src-homology domain 3; C-SH3, C-terminal SH3 domain; Sos, Son of Sevenless; ITC, isothermal titration calorimetry; PDB, Protein Data Bank; H-bond, hydrogen bond; ASA, accessible surface area.

10.1021/bi049752m CCC: $27.50
Published on Web 05/22/2004

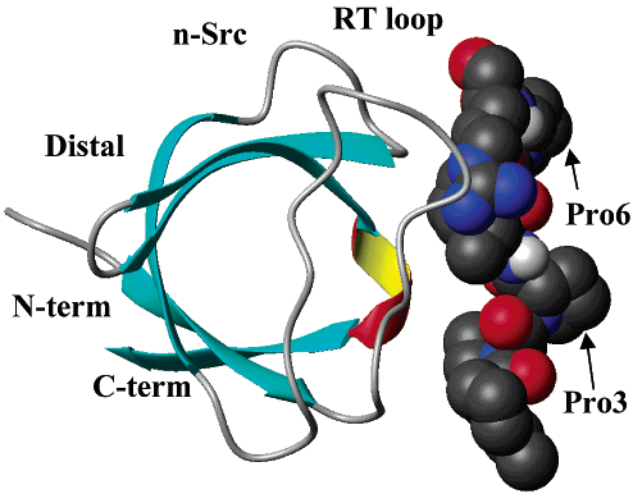

FIGURE 1: Ribbon representation of the crystal structure determined (*16*) of Sem-5 C-SH3 bound to the Sos peptide, Ac−PPPVP-PRRR−NH_2 (CPK model). The major site of interaction between the protein and the peptide consists of the aromatic and acidic residues in the 3_{10} helix and the RT and *n*-src loop regions. The figure was generated from Molmol (*48*).

and purified by the Peptide Synthesis Laboratory (University of Texas Medical Branch). The purity of the peptide (>95%) was checked by mass spectrometry (Louisiana State University) and reverse-phase high-performance liquid chromatography.

ITC. All titration experiments were performed using the Microcal VP-ITC system as described in detail previously (*8*, *9*). For heat capacity determinations, ITC experiments were performed at temperatures from 15 to 35 °C. For pH experiments, the pH ranged from 4.8 to 9. For determination of ΔH_{int}, experiments were performed in different buffers, with protonation enthalpies ranging from 0.12 (acetate buffer) to 11.34 (Tris buffer) (see Table 1) (*14*, *15*). The concentrations of the C-SH3 domain used in the experiments range from 0.3 to 1.2 mM, resulting in final *c* values of 1−17. The SosY peptide concentrations were adjusted such that it was 8−10 times that of the protein concentrations. Data were analyzed using Microcal Origin 5.0 software, fitting the data to the single-site binding model equation to obtain the stoichiometry (*N*), binding constant (K_b), and enthalpy of the binding reaction ($\Delta H°$). The *N* values obtained from the ITC nonlinear least-squares fit range from 1 to 1.2, with an average of 1.1 and standard deviation of 0.05.

Structure-Based Thermodynamic Calculations. Both the crystal structure with the Sos peptide (*16*) and our recently solved solution structure of the unbound C-SH3 domain (*12*) were used in the calculation of the accessible surface areas (ASA). All ASA calculations, on the basis of Lee and Richards method (*17*), were calculated based on thermodynamic parametrization developed by Freire and co-workers (*18*−*31*). In the crystal structure of the bound SH3, two complexes were found in the asymmetric unit, labeled chains A and B. The corresponding peptides in each unit are labeled C and D, respectively. Calculations in this paper utilized the complex consisting of chains A and C. Recalculation of the binding energetics using chains B and D gives $\Delta H = -3500$ cal/mol, $-T\Delta S = -2300$ cal/mol, and $\Delta G = -5800$ cal/mol, which is similar to the results obtained for chains A and C. Structure-based calculations for the apo-protein were performed on the NMR-minimized mean structure (PDB: 1K76) (*12*). To assess the significance of the calculated energetics of the apo-protein, the variation in the values was determined using each member of the experimental ensemble of structures (PDB: 1KFZ). The average difference in the calculated binding enthalpy using the NMR versus the X-ray structure [i.e., $\Delta H_{binding}$(NMR) − $\Delta H_{binding}$(X-ray)] is −8.0 ± 3.0 kcal/mol, indicating that any of the members of the NMR-derived ensemble result in calculated values that are qualitatively similar to the results shown in Figure 5D.

Heat Capacity Change. The heat capacity change associated with protein unfolding from the native state to the denatured state is strongly correlated with changes in the accessible surface area (ΔASA) between the native and unfolded states. This approach has also been found to be applicable to changes associated with binding (*28*). The $\Delta C_{p,binding}$ arises mainly from two contributions: changes in the hydration of apolar and polar groups upon binding and changes in the ionization states (see refs *20*, *32* for details).

Table 1: Binding Energetics of the Association between the Sem-5 C-SH3 Domain and the SosY Peptide Performed under Different pH, Buffer, and Temperature Conditions

peptide[a]	pH	buffer[b]	ΔH_{ion}[c] (kcal mol^{-1})	temp (°C)	K_b[d] (M^{-1})	ΔH_{obs}[d] (kcal mol^{-1})	$\Delta G_{binding}$[d] (kcal mol^{-1})
SosY I	9.0	Tris	11.34	25.1	2.87×10^4	−9.4	−6.1
SosY I	8.5	Tris	11.34	25.1	2.49×10^4	−8.6	−6.0
SosY I	8.0	Tris	11.34	25.1	2.68×10^4	−9.1	−6.0
SosY III	7.5	Tris	11.34	15.2	3.57×10^4	−6.6	−6.0
SosY III	7.5	Tris	11.34	20.2	3.03×10^4	−7.5	−6.0
SosY III	7.5	Tris	11.34	25.1	2.55×10^4	−8.3	−6.0
SosY III	7.5	Tris	11.34	30.1	1.99×10^4	−9.0	−6.0
SosY III	7.5	Tris	11.34	35.2	1.56×10^4	−10.0	−5.9
SosY II	7.5	Tris	11.34	25.1	2.60×10^4	−9.1	−6.0
SosY II	7.5	imidazole	8.75	25.1	2.45×10^4	−8.1	−6.0
SosY II	7.5	Hepes	5.02	25.1	2.43×10^4	−7.6	−6.0
SosY II	7.5	phosphate	1.22	25.1	2.32×10^4	−8.0	−6.0
SosY III	7.0	imidazole	8.75	25.1	2.21×10^4	−8.4	−5.9
SosY III	6.5	imidazole	8.75	25.1	1.85×10^4	−9.3	−5.8
SosY III	4.8	acetate	0.12	25.1	3.03×10^3	−6.7	−4.8

[a] Different SosY (Ac−VPPPVPPRRRY−NH_2) peptide batches used (I−III). [b] Buffer conditions were at 20 mM buffer salt and 200 mM NaCl, except experiments performed at pH 4.8, 50 mM sodium acetate buffer with 100 mM NaCl and 10 mM $CaCl_2$. [c] Values were taken from Fukada and Takahashi (*14*) except for Tris, which was taken from Christensen et al. (*15*). [d] Experimental uncertainties were obtained from the fitting errors and are generally ∼2%.

The first term has been found to be the dominant contribution associated with binding and can be calculated from the following equation:

$$\Delta C_p = 0.45\Delta\mathrm{ASA}_{np} - 0.26\Delta\mathrm{ASA}_{pol} + 0.43\Delta\mathrm{ASA}_{OH}$$

Enthalpy Change. Similarly, the enthalpy change can be parametrized according to ASA changes with an additional term because of the ionization effects. At 60 °C, the median temperature of unfolding for a database of proteins is given by the equation:

$$\Delta H(60\ ^\circ\mathrm{C}) = 31.4\Delta\mathrm{ASA}_{pol} - 8.44\Delta\mathrm{ASA}_{ap} + \Delta\mathrm{H}_{ion}$$

Entropy Change. The entropic changes associated with binding consist of the following dominant contributions: (a) ΔS_{solv}, which arise from the burial of hydrophobic groups upon binding; (b) ΔS_{conf}, conformational changes that occur both for the protein and the ligand in the association reaction. This term is broken down to explicitly account for changes in the backbone conformational entropy (ΔS_{bb}) and changes of the side chain that undergo either initially exposed and then buried from the solvent upon binding ($\Delta S_{bu\rightarrow ex}$) or from the exposed to the unfolded state; (c) ΔS_{trans}, reduction of translational and rotational degrees of freedom; and (d) ΔS_{ion}, changes in the protonation/deprotonation state. This is explicitly stated in the following parametrized equation:

$$\Delta S(T) = \Delta S_{solv}(T) + \Delta S_{conf} + \Delta S_{trans} + \Delta S_{ion}$$

where

$$\Delta S_{solv}(T) = 0.45\Delta\mathrm{ASA}_{ap}\ln(T/384.15) - 0.26\Delta\mathrm{ASA}_{pol}\ln(T/335.15)$$

$$\Delta S_{conf}(T) = \Delta S_{bu\rightarrow ex} + \Delta S_{ex\rightarrow bu} + \Delta S_{bb}$$

$$\Delta S_{bu\rightarrow ex} = \sum_i (\Delta\mathrm{ASA}_i/\mathrm{ASA}_i)\Delta S_{bu\rightarrow ex,T}$$

$$\Delta S_{trans} = 8\ \mathrm{cal\ K^{-1}\ mol^{-1}}$$

Redistribution of the Sos Peptide Ensemble. For the peptide used, the following residues are structured (in P_{II}): $P_1P_2P_3V_4P_5P_6R_7$. The values for κ_{mic} and Δh_{mic}, which were determined previously (*8*) are 0.195 and 1.7 kcal mol^{-1} residue^{-1}, respectively. The degeneracy values used for Ω for each residue (*21*, *24*) are $\Omega_3 = 2.0$, $\Omega_4 = 3.0$, $\Omega_6 = 2.0$, $\Omega_7 = 5.5$. Because positions 1, 2, and 5 are restricted to P_{II} in the WT Sos peptide, $\Omega_1 = \Omega_2 = \Omega_5 = 1.0$. For the P3A− Sos peptide, $\Omega_3 = 7.9$ and $\Omega_2 = 2.0$ (*8*).

RESULTS

Thermodynamics of Binding. The thermodynamics of binding were determined using ITC, which directly measures the heat associated with reactions or processes that occur at constant temperature. From a single binding isotherm (Figure 2A) the enthalpy ($\Delta H_{binding}$), entropy ($\Delta S_{binding}$), and free energy ($\Delta G_{binding}$) changes and stoichiometry (*N*) of the binding reaction can be obtained. Previously, we showed that the binding of Sem-5 to Sos can be approximated as a two-state equilibrium involving the unbound state and a single bound species (*9*). As indicated in Figure 2B, the binding of

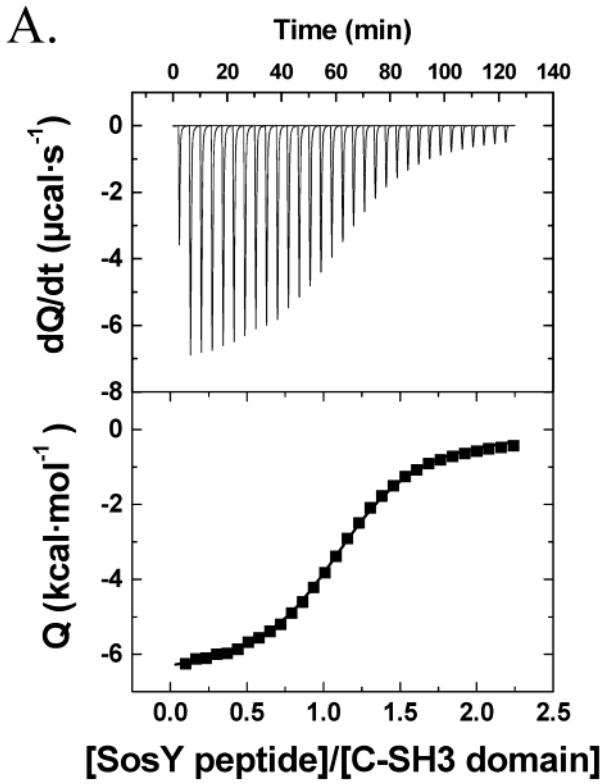

FIGURE 2: (A) Calorimetric titration of the Sem-5 C-SH3 domain with the SosY peptide (Ac−VPPPVPPRRRY−NH_2) in 20 mM Tris and 200 mM NaCl at pH 7.5 and 15 °C. (B) Overall thermodynamic parameters obtained from a fit of the data in A.

Sem-5 C-SH3 to the Sos peptide at pH 7.5 is characterized by a large negative enthalpy ($\Delta H = -8.0 \pm 0.15$ kcal mol^{-1}), which is partially offset by a small negative entropy ($T\Delta S = -2.0 \pm 0.15$ kcal mol^{-1}). Thus, the resultant binding free energy ($\Delta G_{binding} = -6.0$ kcal mol^{-1}) can be categorized as enthalpically driven.

Heat Capacity Change Associated with Binding. ITC experiments were performed in Tris buffer (pH 7.5) at temperatures between 15 and 35 °C to obtain the temperature dependence of $\Delta H_{binding}$ (Table 1). Figure 3 shows the temperature dependence of the binding enthalpy, which decreases linearly with temperature ($R > 0.99$). The slope of the line, which corresponds to the heat capacity change ($\Delta C_{p,binding} = d\Delta H_{binding}/dT$), was determined to be -166 ± 6 cal K^{-1} mol^{-1} and is suggestive of a net burial of the surface (*32*) (see below).

pH Dependence of the Binding Constant. To evaluate the change in the binding constant with pH, ITC experiments were performed at 25 °C between pH 4.8 and 9.0 under the appropriate buffer conditions (Table 1). Although no sig-

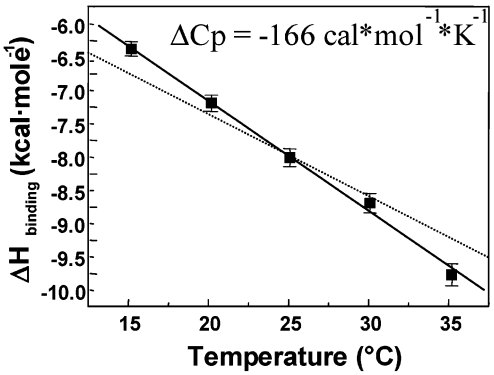

FIGURE 3: Temperature dependence of the binding enthalpy, $\Delta H_{binding}$, for the Sem-5 C-SH3 domain with the SosY peptide at pH 7.5. The slope of the linear least-squares fit (continuous line) yields the heat capacity change associated upon binding, $\Delta C_{p,binding}$, -166 ± 6 cal K^{-1} mol^{-1}. The dashed line represents the calculated heat capacity assuming the NMR structure represents the apo-SEM5 and the binding results in a rigid-body conformational change ($\Delta C_{p,binding}$, -126 cal K^{-1} mol^{-1}). For ease of comparison, the experimental affinity at 25 °C was chosen as the reference.

nificant change in the binding constant is observed from pH 7.5 to 9.0, the binding affinity decreases below pH 6.5, with an approximate 10-fold decrease from pH 6.5 to 4.8. As noted previously (*32*), the decrease in binding affinity with decreasing pH is indicative of a release in protons upon complex formation and can be described quantitatively using Wyman's linkage relationship

$$n_{H^+} = \frac{\partial \ln K_b}{2.303\ \partial\ \mathrm{pH}} \quad (1)$$

where n_{H^+} is the number of protons that become associated/dissociated from the protein upon complex formation. The absence of a pH dependence above pH 7.5 indicates the binding is not coupled to proton release/uptake at neutral pH. Further support for this conclusion is that ITC experiments were conducted at pH 7.5 and 25 °C using four different buffers (phosphate, Hepes, imidazole, and Tris), each with different ionization enthalpies, ΔH_{ion} (1.22−11.34 kcal mol^{-1}). As described previously (*32*), the apparent binding enthalpy consists not only of the intrinsic enthalpy of the binding reaction, but also a term that is dependent on the buffer contributions as summarized by the following equation:

$$\Delta H_{binding} = \Delta H_{int} + n_{H^+}\,\Delta H_{ion} \quad (2)$$

where n_{H^+} is the number of protons added or released (if $n_{H^+} > 0$) by the buffer and associated with the protein. The relative independence of the $\Delta H_{binding}$ on ΔH_{ion} for the different system buffers (Table 1) indicates that the binding reaction at pH 7.5 is not coupled to a protonation equilibrium and that the observed binding constant of $\sim 2.4 \times 10^4$ M^{-1} and enthalpy change of ~ -8 kcal mol^{-1} at pH 7.5 are not monitoring protonation effects.

DISCUSSION

Structural Thermodynamic Analysis. Because the thermodynamics of binding of Sem-5 to Sos are not coupled to protonation at neutral pH, as noted above, pH 7.5 was chosen as a reference condition to evaluate the relative determinants of binding. The experimentally observed free energy of binding for Sem-5 C-SH3 ($\Delta G = -6.0$ kcal mol^{-1} at pH 7.5) is similar to that obtained for the binding of the human homologue Grb2 N-SH3 domain to mSos (*10*), the binding of c-Src to the RLP2 peptide (*5*), and the binding of the Fyn SH3 domain to the P2L peptide (PPRPLPVAPGSSKT) (*6*). Also consistent with other SH3 domains is the large negative enthalpy of binding (*2*, *5*, *6*, *10*). However, despite the agreement between the experimental values obtained for different SH3 domains, it has been asserted that it is difficult to rationalize the observed energetics in the context of the surface area that is buried at the binding interface (*5*). The fact that the binding interface is primarily hydrophobic is recognized upon inspection of Figure 4, which shows the residues in Sem-5 and the Sos peptide that bury surface area in the complex. As is the case with other SH3 domains, the binding interaction in Sem-5 is predominantly mediated through hydrophobic interactions between aromatic and aliphatic atoms of Sem-5 (e.g., TRP191, TYR207, and PHE165) and the Pro residues of the Sos peptide (Figure 1).

To evaluate quantitatively the difference between the thermodynamics that are expected from the hydrophobic binding site and the experimentally observed energetics (Figure 2B), the surface-area-based parametrization of the energetics of Freire and co-workers (*18*−*31*) was utilized. According to this parametrization, the heat capacity ΔC_p, enthalpy, ΔH, and solvation entropy, ΔS_{solv}, changes can be estimated from the changes in the solvent-accessible polar and apolar surface area upon binding or folding (see the Materials and Methods). Although such an approach is clearly an approximation, previous successes of the energetic parametrization (*32*, *33*) indicate that it is indeed an effective means of estimating the energetic consequences of surface area burial upon binding. To evaluate the energetic contribution of the binding interface *only*, the thermodynamics were calculated using the high-resolution X-ray structure of the complex (*16*) and calculating the accessible surface area with and without the ligand. Such a scenario, although unrealistic, provides a means of identifying the energetic impact of only the residues that are in direct contact with the ligand (Figure 4). Because the majority of surface area that is buried in the complex is apolar ($\Delta ASA_{ap} = -257$ Å^2 versus $\Delta ASA_{pol} = -155$ Å^2), the corresponding calculated energetics yield a $\Delta H = 1850$ cal mol^{-1} and $T\Delta S = 6000$ cal mol^{-1} (parts A and B of Figure 5). The large positive entropy and small positive enthalpy of binding result primarily from the burial of the hydrophobic surface, and these results are consistent with the binding energetics obtained experimentally for systems that are known to be mediated through hydrophobic interactions (*34*).

Despite the predominantly hydrophobic nature of the binding site of Sem-5 and other SH3 domains (*3*, *7*, *16*, *35*−*39*), the experimentally observed binding energetics (Figure 2B) reveal enthalpy and entropy values that are dramatically different from what is expected of a primarily hydrophobic interaction (compare Figure 2B with Figure 5B). Indeed, the predicted enthalpy and entropy are of opposite signs from the experimentally observed values. On the basis of the previous success of the structural energetic parametrization at predicting protein stabilities, binding affinities, and capturing details of the native state ensemble (*18*−*31*, *40*−*43*), it

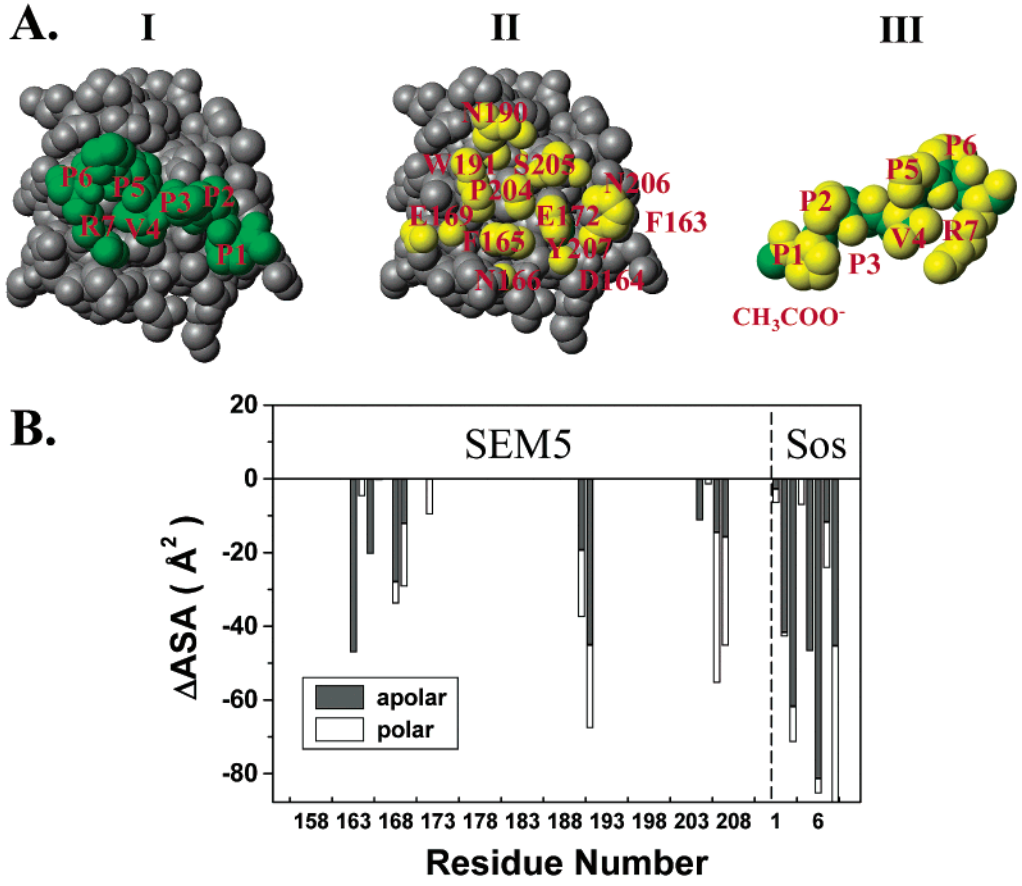

FIGURE 4: (A) I. CPK model representation of the crystal structure determined (*16*) of Sem-5 C-SH3 (gray) bound to the Sos peptide Ac−PPPVPPRRR−NH_2 (green). II. Same as A but without the Sos peptide. The yellow highlights the residues that are buried upon ligand binding. III. Sos peptide alone (rotated 180° relative to the position in I). Residue labels are shown for the peptide and the residues of the protein that are buried by the peptide. (B) Changes in polar and apolar accessible surface areas (ΔASA) upon complex formation for both Sem-5 C-SH3 and the ligand Sos peptide.

is unlikely that the significant disagreement in both magnitude and sign between the calculation and experiment is due to the calculation itself. In fact, the discrepancy between the experiment and expectation for the binding energetics of SH3 domains has been noted by other groups and is not predicated on the structural-energetic parametrization used here (*2*, *5*, *6*).

Energetics of Structural Rearrangements in Sem-5. The quantitative estimates in Figure 5B reveal that in addition to changes at the binding interface, other thermodynamic determinants must exist, which significantly impact the observed energetics. Because the contributions due to protonation have been experimentally ruled out, as described above, the contributions must arise from structural and dynamic changes to the protein and/or peptide.

Recently, we determined the high-resolution NMR solution structure of the Sem-5 C-SH3 domain in the absence of the Sos peptide (*12*). Analysis of the structure revealed several differences between the unbound Sem-5 C-SH3 and the Sem-5−Sos complex (*12*), and many of those differences are shared with other SH3 domains (*39*, *44*). Most notable are the differences in the RT and distal loops and the residues comprising the aromatic binding surface of the 3_{10} helix (*12*). To obtain a quantitative estimate of the energetic consequences of the observed structural differences, the binding affinity for Sos was calculated assuming an equilibrium in which binding is coupled to a rigid-body conformational change [i.e., the unbound Sem-5 can be represented by the average NMR structure of the apo-protein (*12*) and the bound Sem-5 can be represented by the X-ray structure of the complex (*16*)]

$$\text{Apo-Sem-5(NMR)} + \text{Sos} \rightleftarrows \text{Sem-5}-\text{Sos(X-ray)}$$

The resultant residue-specific and overall energetics are shown in parts C and D of Figure 5, respectively. Several observations can be made when comparing parts A and B of Figure 5 to parts C and D of Figure 5. First, the structural difference between the free and complexed Sem-5 reported previously has a significant effect on the predicted thermodynamics of binding. Of special note is the fact that many residues, not just those in the binding site, contribute to the binding energy, because of the conformational rearrangements in the protein. Second, the magnitudes of estimates, which consider the structural rearrangements, differ significantly from the estimates derived from the binding site alone (Figure 4). In particular, the sign of the binding enthalpy is negative, owing to changes in the polar surface area as a result of the structural changes in Sem-5 (Figure 5D). In other words, although the binding interface is dominated by apolar interactions (Figure 4), the net contribution of the local and global structural changes in the protein upon binding are heavily influenced by changes in the polar surface. As noted previously (*12*), the agreement between the structural changes observed upon binding in the Sem-5 system and the structural changes observed in other systems (*39*, *44*) suggests that the

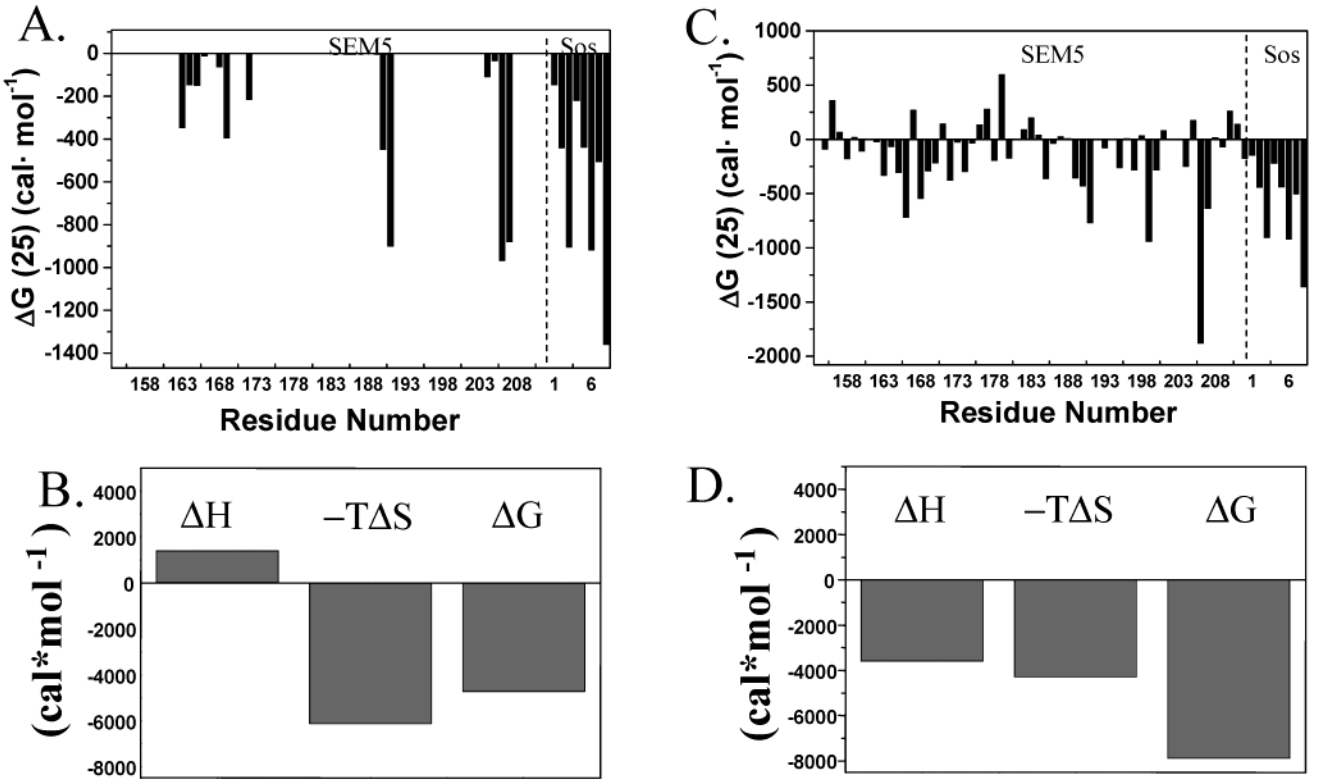

FIGURE 5: Free energy of binding calculated with the surface-area-based parametrization of the energetics described in the Materials and Methods. (A) Estimate of the residue-specific contributions to the free energy of binding from the binding interface alone. Values were determined using the surface area burial from the crystal structure of the complex (*16*), assuming no structural rearrangements. (B) Overall energetics calculated from the individual contributions shown in A. (C) Residue-specific contributions to the free energy of binding assuming the bound state is the X-ray structure of the complex and the unbound state is the NMR structure of the apo-Sem-5 (*11*) (see text for details). (D) Overall energetics calculated from the individual contributions shown in C. All calculations are shown at 25 °C. The contributions in B and D do not include the cratic entropy term (see the Materials and Methods), which cannot be attributed to specific residues.

observed differences are not artifacts unique to Sem-5 and that global structural changes play a significant role in determining the overall energetics of binding between the SH3 domains and their putative targets. Indeed, previous work by Nicholson and colleagues has implicated structural changes throughout the protein as being a plausible explanation for the proposed discrepancy between the experiment and expectation (*5*).

Of note is that the X-ray structure of the holo-SEM5 was determined at pH 8.0, whereas the NMR solution of the apo-SEM5 was determined at pH 4.8. Although these solution conditions differ dramatically, a comparison of the chemical shift differences of the apo-protein as a function of pH (titrating from 8.4 to 2.0) indicates that, except for the immediate environment around titratable residues, the chemical shifts for the majority of residues, particularly in regions of the molecule where structural differences between the apo and holo forms of the molecule were noted (*12*), do not change (not shown), indicating that the global structural changes that are observed between the apo and holo forms of the molecule are not following a pH-induced conformational change.

Although the agreement between the experimental thermodynamics and those calculated by considering an association coupled to a rigid-body conformational change represents an improvement over the static model (Figure 2B versus parts B and D of Figure 5), this representation of the equilibrium, nonetheless, does not capture the magnitude of the entropy and enthalpy of binding and consequently the free energy, as shown in Figure 6. In particular, the experimental binding affinity is less than the surface-area-based estimate ($\Delta G_{binding}$(exp) = −6.0 kcal mol^{-1} versus $\Delta G_{binding}$(calcd) = −7.8 kcal mol^{-1}), and more strikingly, the experimental enthalpy of binding is significantly lower than the surface area prediction ($\Delta H_{binding}$(exp) = −7.8 kcal mol^{-1} versus $\Delta H_{binding}$(calcd) = −3.8 kcal mol^{-1}). In addition, the experimental $\Delta C_{p,binding}$ (Figure 3) is significantly more negative than the value calculated from the changes in the surface area accompanying the binding, assuming the rigid-body structural change modeled in parts C and D of Figure 5 ($\Delta C_{p,binding}$(exp) = −166 ± 15 cal K^{-1} mol^{-1} versus $\Delta C_{p,binding}$(pred) = −126 cal K^{-1} mol^{-1}).

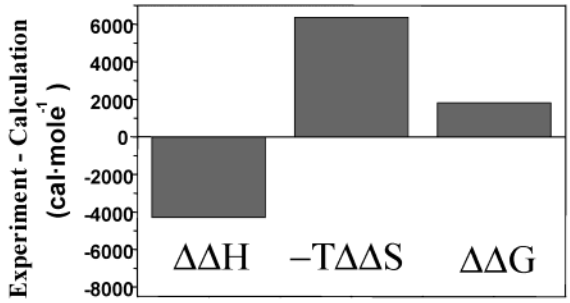

FIGURE 6: Difference between the experimental (Figure 2B) and computed (Figure 5D) thermodynamic parameters [ΔX(exp) − ΔX(calcd)] for the binding of Sem-5 to Sos at 25 °C.

The lack of agreement between the calculated and experimental energetics (Figure 6) has two important im-

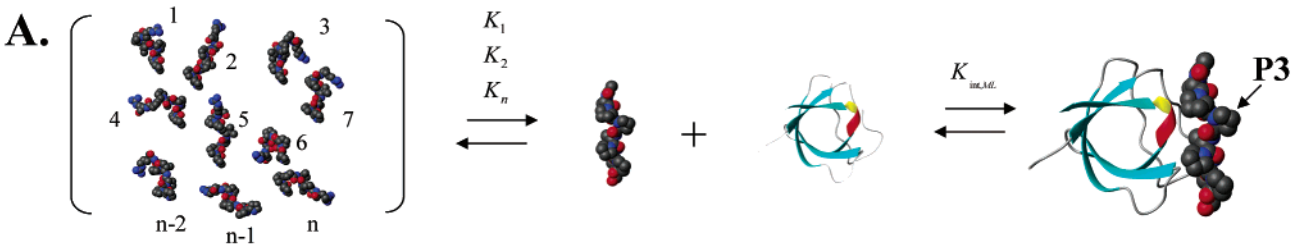

B.

$$K_{bind} = \frac{[MP]}{[M][P_{tot}]} = \frac{[MP]}{[M][P_{free}]\left(1 + \sum_{i=1}^{n_{conf\_P}} K_i\right)}$$

$$K_{bind} = \frac{K_{\mathrm{int},MP}}{\left(1 + \sum_{i=1}^{n_{conf\_P}} K_i\right)} = \frac{K_{\mathrm{int},MP}}{Q_{conf,P}}$$

$$-RT \ln K_{bind} = -RT \ln K_{\mathrm{int},MP} + RT \ln Q_{conf,P}$$

$$\Delta G_{binding} = \Delta G_{\mathrm{int},MP} - \Delta G_{conf,P}$$

FIGURE 7: (A) Binding equilibrium involving a conformational manifold of the Sos peptide. The association process consists of the redistribution of the conformational ensemble from the binding-incompetent (in brackets) to binding-competent (P_{II}) species. SWs of the individual conformational states 1, 2, 3, ..., *n* are K_1, K_2, K_3, ..., K_n, respectively. (B) Linkage relationship describing the impact of the conformational equilibrium for the peptide on the observed binding energetics.

plications. First, it provides quantitative estimates of the discrepancy which has, to date, been described only in qualitative energetic terms (*5*). Second, it indicates that neither the binding interface alone, nor the structural changes in the protein that accompany binding, provides a complete representation of the determinants for the association process. Consequently, additional factors not previously considered are likely to significantly impact the binding thermodynamics in SH3 domains.

Thermodynamics of Formation of the P_{II} Conformation by the Sos Peptide. For equilibrium processes, such as the association of Sem-5 with Sos, wherein a protein interacts with the peptide ligand, the peptide is believed to be unstructured in the unbound state and the binding reaction is coupled to the folding of the peptide (Figure 7). In other words, in the absence of the Sem-5 binding partner, the Sos peptide exists as an ensemble of interconverting conformational states, only a subset of which are competent to bind Sem-5. Upon binding, the ensemble is redistributed to the binding competent form(s). In the case of the Sos peptide, the binding competent state is the left-handed P_{II} conformation. Thus, the overall binding equilibrium can be viewed as two separate equilibrium processes; one describing the conformational equilibrium of the peptide and the other describing the binding between the P_{II} conformation of the peptide and the Sem-5 molecule (Figure 7B). If the Sos peptide is prefolded to P_{II} in the unbound state, the conformational free energy (i.e., $\Delta G_{\mathrm{conf,P}} = -RT \ln[1 + \Sigma K_i]$) is ~0 and the observed binding free energy simply corresponds to the intrinsic binding energy (i.e., $\Delta G_{\mathrm{bind}} = \Delta G_{\mathrm{int,MP}}$). If, on the other hand, the peptide is populating a disordered or random-coil state, the overall binding free energy will be the difference between the intrinsic binding energy and the energy required to fold the peptide into the P_{II} conformation from the myriad of non-P_{II} conformations. A significant goal therefore is to be able to separate the energetic effects associated with conformational redistribution of the peptide ensemble from the intrinsic binding energy.

To facilitate a characterization of the energetics of folding the Sos peptide into the P_{II} conformation, we consider the following: Previous studies in our laboratory have demonstrated that Ala and Gly substitutions at the surface exposed 3rd and 6th positions in the Sos peptide (Figure 1) results in a decrease in binding affinity, even though the side chains of the mutated residues do not make contact with Sem-5 in the bound complex (*8*). As described in that paper, the origin of the difference in binding affinity is due to the difference in the extent to which each amino acid is biased toward the P_{II} conformation in the unbound state. Interestingly, it was demonstrated that the physical basis for the bias could be approximated as being identical for Pro, Ala, and Gly but that the rank order in the bias (i.e., Pro > Ala > Gly) is inversely related to the degeneracy of non-P_{II} conformations. In other words, the higher degeneracy for Gly in the unbound state will shift the equilibrium away from the P_{II} conformation. A direct consequence of this result is that the per residue equilibrium constant (K_i) between the P_{II} state and the ensemble of non-P_{II} conformations can be expressed as a product of two terms: the degeneracy (Ω_i) of all non-P_{II} conformations (Figure 8), which is residue-specific (*8*, *45*) and the microscopic P_{II} bias, κ_{mic}, which is common to all amino acids

$$K_i = \Omega_i \, \kappa_{\mathrm{mic}}$$

The importance of this equality is that it provides a means of explicitly calculating the conformational free energy terms for the Sos peptide. This is shown in Figure 8, where the ensemble of conformational states of the peptide ($Q_{\mathrm{conf,P}}$) consists of all possible combinations for each amino acid to be in either the P_{II} conformation (P) or the disordered/non-P_{II} conformation (U). The statistical weight (SW) of each conformational state is therefore, the product of all κ_{mic} and

State No.	Conformation	Statistical Weight (SW)	
0	$P_1P_2P_3P_4P_5P_6P_7$	1	1
1	$\boldsymbol{U_1}P_2P_3P_4P_5P_6P_7$	K_1	$\Omega_1\kappa_{mic}$
2	$\boldsymbol{U_1U_2}P_3P_4P_5P_6P_7$	K_1K_2	$\Omega_1\Omega_2\kappa_{mic}^2$
3	$\boldsymbol{U_1}P_2\boldsymbol{U_3}P_4P_5P_6P_7$	K_1K_3	$\Omega_1\Omega_3\kappa_{mic}^2$
.	.	.	.
$2^{Nres}-1$	$\boldsymbol{U_1U_2U_3U_4U_5U_6U_7}$	$K_1K_2K_3K_4K_5\ K_6K_7$	$\prod_i^{N_i}\Omega_i \cdot \kappa_{mic}^{N_i}$

$$Q_{conf,P} = \sum_{j=1}^{n_{states}} SW_j$$

$$Q_{conf,P} = \prod_{i=1}^{N_{residj}} (1 + \Omega_i \cdot \kappa_{mic}) \qquad where \qquad \kappa_{mic} = e^{\frac{-\Delta h_{mic}}{RT} + \frac{\Delta s_{mic}}{R}}$$

$$Q_{conf,P} = (1+\Omega_{PRO1}\cdot\kappa_{mic})(1+\Omega_{PRO2}\cdot\kappa_{mic})(1+\Omega_{PRO3}\cdot\kappa_{mic})(1+\Omega_{VAL4}\cdot\kappa_{mic})(1+\Omega_{PRO5}\cdot\kappa_{mic})(1+\Omega_{PRO6}\cdot\kappa_{mic})(1+\Omega_{ARG7}\cdot\kappa_{mic})$$

FIGURE 8: Schematic representation of the conformational partition function for the Sos peptide. The individual states in the conformational ensemble involve all possible combinations for each residue to be in either the P_{II} or non-P_{II} state. The partition function for the ensemble is the sum of the SWs, which can be represented by the binomial expansion of the microscopic κ_{mic} (see text). Values for the degeneracy of each residue were determined elsewhere (*21*, *24*) and are listed in the Materials and Methods.

degeneracy terms (Ω_i) at each position. If no P_{II} bias exists (i.e., $\kappa_{mic} = 1$), the SW is determined only by the degeneracy and the ensemble corresponds to a random coil. If, on the other hand, a P_{II} bias exists (i.e., $\kappa_{mic} < 1$), the SW for adopting a non-P_{II} conformation will be decreased and the conformational free energy of folding the peptide into the binding competent conformation will likewise be decreased.

The ability to describe the thermodynamics of adopting the P_{II} conformation in terms of a background energetic contribution for each amino acid provides a means of dramatically simplifying the conformational free energy of the peptide. For such a case, the conformational partition function of the Sos peptide ($Q_{conf,P}$) can be approximated by a binomial expansion of the energetic bias at each position, and the overall energy of adopting the non-P_{II} conformation becomes

$$\Delta G_{conf,P} = -RT \ln Q_{conf,P}$$

$$\Delta G_{conf,P} = -RT \ln[\prod_{i=1}^{N_{res}} (1 + \Omega_i \kappa_{mic})] \qquad (3)$$

where the product is over all residues in the Sos peptide that adopt the P_{II} conformation upon binding (i.e., residues 1−7) (*16*). Thus, determination of the conformational free energy contribution to binding is predicated by knowing the value of κ_{mic} as well as Ω_i at each position.

Recently (*8*, *45*), the experimentally observed difference in binding affinity between Sem-5 and the Sos peptide with either Pro at position 3 (P3−Sos) or Ala at position 3 (P3A−Sos) was used to determine the value of the microscopic (i.e., per residue) equilibrium constant for P_{II} unfolding ($\kappa_{mic} = 0.195$) as well as the microscopic enthalpy of unfolding ($\Delta h_{mic} = 1.7$ kcal mol^{-1} residue^{-1}). Deriving the expressions for the component enthalpy ($\Delta H_{conf,P}$) and entropy ($\Delta S_{conf,P}$) functions for the conformational transition from P_{II} (by taking the appropriate temperature derivatives of eq 3) gives

$$\Delta H_{conf,P} = -R \frac{\partial \ln Q_{conf,P}}{\partial (1/T)} = \sum_{i=1}^{7} \frac{\Omega_i \kappa_{mic}}{Q_{conf,P}} \Delta h_{mic} \qquad (4)$$

and

$$\Delta S_{conf,P} = -R \frac{\partial (T \ln Q_{conf,P})}{\partial (T)} = -R \ln Q_{conf,P} - \sum_{i=1}^{7} \frac{\Omega_i \kappa_{mic}}{T Q_{conf,P}} \Delta h_{mic} \qquad (5)$$

Substituting for κ_{mic}, Δh_{mic}, and Ω_i for each residue provides a quantitative solution to the thermodynamics associated with the folding of the peptide into the P_{II} conformation. We note that the backbone Ω_i values for each residue were taken from the conformational entropy estimates ($\Delta S = R \ln \Omega_i$), determined previously for each amino acid (*21*, *33*), and κ_{mic} and Δh_{mic} were determined previously (*45*) (see the Materials and Methods).

Thermodynamics Signature of P_{II} Folding. Figure 9A shows the thermodynamics associated with prefolding the Sos peptide into the P_{II} conformation, which reflects the energetic impact that would be observed on the measured thermodynamics of binding. The negative enthalpy and entropy, coupled with the positive free energy indicates that folding into the P_{II} conformation results in a sizable release of heat $\Delta H_{conf,P} = -2500$ cal mol^{-1}, as well as a significant decrease in entropy. Relative to an interaction between a prefolded P_{II} helix and Sem-5, the observed enthalpy and entropy functions would be significantly more negative and the free energy would be more positive. Interestingly, the

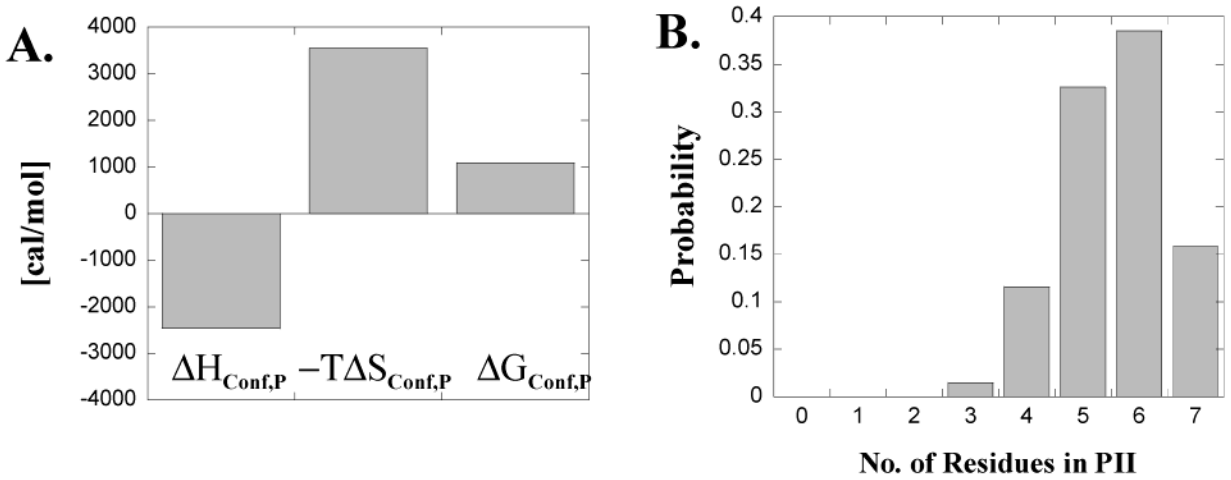

FIGURE 9: (A) Energetics associated with redistributing the Sos peptide conformational ensemble to the binding competent P_{II} conformation upon binding. (B) Probability of finding different numbers of residues in the P_{II} conformation in the Sos conformational ensemble. B indicates that the ensemble is significantly biased toward P_{II} in the unbound state. Despite the significant P_{II} bias, A reveals that the energetics associated with completely folding the ensemble to P_{II} are significant.

thermodynamic signature (defined here as the sign of the enthalpy, entropy, and free energy functions) for P_{II} folding is similar to the signature obtained from the difference between the experimental and calculated thermodynamics (Figure 6). The importance of this agreement stems from fact that, within the context of the surface-area-based parametrization used here, the enthalpy of folding the Sos peptide into the P_{II} conformation should only amount to -75 cal mol^{-1} because the surface area burial upon folding to the P_{II} state from the unfolded state is minimal. In effect, the structural energetic parametrization does not capture the energetics associated with P_{II} folding. If it is the case that the parametrization captures all but the P_{II} folding, the difference between the experimental and calculated values should correspond to the signature for the unaccounted energetics. The fact that the signatures are indeed similar is thus intriguing. It should be noted, however, that the magnitudes of the effects shown in Figure 9A are less than the signature values in Figure 6 and suggest that the energetic consequences of P_{II} folding are not likely to be the sole source of the discrepancy between the prediction and experiments. Along these lines, our laboratory has recently shown (*9*, *12*) that a decrease in the conformational fluctuations in the RT loop of Sem-5 is also likely to impact the energetics of binding between Sem-5 and Sos in much the same way as the P_{II} folding described. Namely, structuring of the RT loop upon binding is predicted [on the basis of a folding/unfolding model of fluctuations (*12*, *40*)] to produce a thermodynamic signature, which is also similar to Figure 6, but like the P_{II} energetics, predicts values that are lesser in magnitude than those shown in Figure 6. When taken together, the results presented here and previously (*12*) suggest that conformational redistribution in both the protein and the peptide ensembles contributes substantially to the thermodynamics of binding.

Conformational Partition Function for the Sos Peptide Ensemble. The picture of the Sos peptide conformational ensemble that emerges from this analysis is noteworthy. The fact that each amino acid has an intrinsic P_{II} bias (*8*) means that, even in the unbound state, the peptide ensemble is heavily biased toward conformations with a significant number of residues in P_{II}. From the partition function shown in Figure 8, the probability of finding a molecule with a certain number of residues in the P_{II} conformation can be expressed as

$$P(7\mathrm{P_{II}}) = \frac{1}{Q_{\mathrm{conf,P}}}$$

$$P(6\mathrm{P_{II}}) = \frac{\kappa_{\mathrm{mic}} \sum_{i=1}^{n_{\mathrm{Nres}}} (\Omega_3 + \Omega_4 + \Omega_6 + \Omega_7)}{Q_{\mathrm{conf,P}}}$$

$$P(5\mathrm{P_{II}}) = \frac{\kappa_{\mathrm{mic}}^{\,2} \sum_{i=1}^{n_{\mathrm{Nres}}} ((\Omega_3\Omega_4) + (\Omega_3\Omega_6) + (\Omega_3\Omega_7) + (\Omega_4\Omega_6) + (\Omega_4\Omega_7) + (\Omega_6\Omega_7))}{Q_{\mathrm{conf,P}}}$$

$$P(4\mathrm{P_{II}}) = \frac{\kappa_{\mathrm{mic}}^{\,3} \sum_{i=1}^{n_{\mathrm{Nres}}} ((\Omega_3\Omega_4\Omega_6) + (\Omega_3\Omega_4\Omega_7) + (\Omega_3\Omega_6\Omega_7) + (\Omega_4\Omega_6\Omega_7))}{Q_{\mathrm{conf,P}}}$$

$$P(3\mathrm{P_{II}}) = \frac{\kappa_{\mathrm{mic}}^{\,4} \sum_{i=1}^{n_{\mathrm{Nres}}} (\Omega_3\Omega_4\Omega_6\Omega_7)}{Q_{\mathrm{conf,P}}}$$

Although the significant overall bias (Figure 9B) is due in part to the fact that residues 1, 2, and 5 are restricted to P_{II} by the Pro residues immediately following (i.e., $P(2\mathrm{P_{II}}) = P(1\mathrm{P_{II}}) = P(0\mathrm{P_{II}}) = 0$) (*46*, *47*), even the residues that are capable of occupying other conformations are nonetheless occupying the P_{II} conformation for a significant fraction of the time. In fact, the results determined here suggest that ~15% of the peptide molecules are completely folded in the P_{II} conformation at any instance (i.e., all residues are P_{II}), whereas only ~2% of the molecules have all of the residues that are capable of adopting non-P_{II} conformations actually in those non-P_{II} conformations simultaneously.

In summary, Figure 9 reveals that the energy associated with folding the Sos peptide into the P_{II} conformation has a dramatic effect on the overall energetics of binding. Upon binding, the distribution shown in Figure 9B shifts to the right, completely populating the P_{II} state (assuming no other conformational state can bind to Sem-5). The energetic parameters shown in Figure 9A thus are not the energetics associated with folding a random-coil ensemble into a folded conformation. On the contrary, the energetic parameters represent folding of an already significantly biased ensemble toward the fully P_{II} state. The fact that such dramatic energetic consequences arise from such a relatively small population shift highlights the importance of thermodynamic changes that must accompany dynamic changes in this system. Such changes may, as is the case here, be missed or incorrectly accounted for by simple inspection of the canonical structure or even by surface-area-based calculations.

It is important to point out that, while the partition function for the peptide shown in Figure 8 is valid if the P_{II} folding/unfolding reaction is indeed noncooperative, the validity of the calculated energetics depends on the accuracy of κ_{mic} and the degeneracy terms for each amino acid. Because the κ_{mic} term is valid for Ala and does not include energetic contributions of side chains, it is likely that the energetic contributions for larger amino acids will affect the quantitative results presented here. Nonetheless, such differences are not likely to impact the qualitative conclusions. Because P_{II} appears to be a dominant conformation for most amino acids (*47*) and because the source of the P_{II} bias is enthalpic, it is likely that all unstructured peptides and proteins will be at least partially biased toward P_{II} and further folding to P_{II} will result in a net positive heat effect. As such, the similarity between the thermodynamic signature for P_{II} folding (Figure 9A) and the noted discrepancy between the experimental and expected binding energetics of SH3 domains (Figure 6) is likely to persist.

Finally, another significant point that emerges from the analysis of the energetics of P_{II} formation in the Sos peptide is that the effect of the folding on the free energy function is significantly less than the effects on the enthalpy and entropy functions. This indicates that the free energy alone does not provide a suitable description of the determinants of binding in this system and that the accuracy of the free energy prediction (without explicit consideration of the component enthalpy and entropy functions) is not a reliable metric of the predictive method. Instead, an accurate assessment of the physical determinants of binding requires insight into the component enthalpy and entropy functions, which illuminate the thermodynamic mechanism and therefore vary to a much greater extent than the free energy.

CONCLUSION

The observation that the binding of SH3 domains to their putative peptide targets is characterized by large negative enthalpies, even though the apolar binding interfaces would predict positive enthalpy changes, has long been recognized as a conundrum (*2*, *5*, *6*, *10*). Here, we have investigated the quantitative impact of folding the peptide into the binding competent conformation (P_{II}) on the observed energetics and find that the effects (1) are significant in magnitude, (2) are of the same sign that would be needed to explain the discrepancy, and (3) are difficult to reconcile in the context of surface area burial upon folding. These results represent the first quantitative thermodynamic description of the impact of the P_{II} bias in unstructured peptides on the thermodynamics of interaction between SH3 domains and their peptide targets.

ACKNOWLEDGMENT

The authors thank Steve Whitten, Allan Ferreon, and Wayne Bolen for helpful discussions and Xiao Lian Liang for assistance with the overexpression of the protein used in this paper.

REFERENCES

1. Weber, G. (1992) *Protein Interactions*, Chapman and Hall, London, U.K.
2. Arold, S., O'Brien, R., Franken, P., Strub, M., Hoh, F., Dumas, C., and Ladbury, J. E. (1998) RT Loop Flexibility Enhances the Specificity of Src Family SH3 Domains for HIV-1 Nef, *Biochemistry 37*, 14683−14691.
3. Ladbury, J. E., and Arold, S. (2000) Searching for specificity in SH domains, *Chem. Biol. 7*, R3−R8.
4. Lee, C., Leung, B., Lemmon, M. A., Zheng, J., Cowburn, D., Kuriyan, J., and Saksela, K. (1995) A single amino acid in the SH3 domain of Hck determines its high affinity and specificity in binding to HIV-1 Nef protein, *EMBO J. 14*, 5006−5015.
5. Wang, C., Pawley, N. H., and Nicholson, L. K. (2001) The Role of Backbone Motions in Ligand Binding to the c-Src SH3 Domain, *J. Mol. Biol. 313*, 873−887.
6. Renzoni, D. A., Pugh, D. J. R., Siligardi, G., Das, P., Rossi, C., Waterfield, M. D., Campbell, I. D., and Ladbury, J. E. (1996) Structural and Thermodynamic Characterization of the Interaction of the SH3 Domain from Fyn with the Proline-Rich Binding Site on the p85 Subunit of P13-Kinase, *Biochemistry 35*, 15646−15653.
7. Pisabarro, M. T., Serrano, L., and Wilmanns, M. (1998) Crystal Structure of the Abl-SH3 Domain Complexed with a Designed High-Affinity Peptide Ligand: Implications for SH3−Ligand Interactions, *J. Mol. Biol. 281*, 513−521.
8. Ferreon, J. C., and Hilser, V. J. (2003) The effect of the polyproline II (PPII) conformation on the denatured state entropy, *Protein Sci. 12*, 447−457.
9. Ferreon, J. C., and Hilser, V. J. (2003) Ligand-induced changes in dynamics in the RT loop of the C-terminal SH3 domain of SEM-5 indicate cooperative conformational coupling, *Protein Sci. 12*, 982−996.
10. Wittekind, M., Mapelli, C., Farmer, B. T., II, Suen, K., Goldfarb, V., Tsao, J., Lavoie, T., Barbacid, M., Meyers, C. A., and Mueller, L. (1994) Orientation of Peptide Fragments from Sos Proteins Bound to the N-Terminal SH3 Domain of Grb2 Determined by NMR Spectroscopy, *Biochemistry 33*, 13531−13539.
11. Egan, S. E., Giddings, B. W., Brooks, M. W., Buday, L., Sizeland, A. M., and Weinberg, R. A. (1993) Association of Sos Ras exchange protein with Grb2 is implicated in tyrosine kinase signal transduction and transformation, *Nature 363*, 45−51.
12. Ferreon, J. C., Volk, D. E., Luxon, B. A., Gorenstein, D. G., and Hilser, V. J. (2003) Solution Structure, Dynamics, and Thermodynamics of the Native State Ensemble of the Sem-5 C-terminal SH3 Domain, *Biochemistry 42*, 5582−5591.
13. Wittekind, M., Mapelli, C., Lee, V., Goldfarb, V., Friedrichs, M. S., Meyers, C. A., and Mueller, L. (1997) Solution Structure of the Grb2 N-terminal SH3 Domain Complexed with a Ten-Residue Peptide Derived from SOS: Direct Refinement Against NOEs, J-couplings, and ^{1}H and ^{13}C Chemical Shifts, *J. Mol. Biol. 267*, 933−952.
14. Fukada, H., and Takahashi, K. (1998) Enthalpy and heat capacity changes for the proton dissociation of various buffer components in 0.1 M potassium chloride, *Proteins: Struct., Funct., Genet. 33*, 159−166.
15. Christensen, J. J., Hansen, L. D., and Izatt, R. M. (1976) *Handbook of Proton Ionization Heats*, John Wiley and Sons, New York.

16. Lim, W. A., Richards, F. M., and Fox, R. O. (1994) Structural determinants of peptide-binding orientation and of sequence specificity in SH3 domains, *Nature 372*, 375−379.
17. Lee, B., and Richards, F. M. (1971) The interpretation of protein structures: Estimation of static accessibility, *J. Mol. Biol. 55*, 379−400.
18. Bardi, J. S., Luque, I., and Freire, E. (1997) Structure-based thermodynamic analysis of HIV-1 protease inhibitors, *Biochemistry 36*, 6588−6596.
19. Luque, I., Mayorga, O. L., and Freire, E. (1996) Structure-based thermodynamic scale of α-helix propensities in amino acids, *Biochemistry 35*, 13681−13688.
20. Hilser, V. J., Gomez, J., and Freire, E. (1996) The enthalpy change in protein folding and binding: Refinement of parameters for structure-based calculations, *Proteins: Struct., Funct., Genet. 26*, 123−133.
21. D′Aquino, J. A., Gomez, J., Hilser, V. J., Lee, K. H., Amzel, L. M., and Freire, E. (1996) The magnitude of the backbone conformational entropy change in protein folding, *Proteins 25*, 143−156.
22. Gomez, J., Hilser, V. J., Xie, D., and Freire, E. (1995) The heat capacity of proteins, *Proteins: Struct., Funct., Genet. 22*, 404−412.
23. Xie, D., and Freire, E. (1994) Structure based prediction of protein folding intermediates, *J. Mol. Biol. 242*, 62−80.
24. Lee, K. H., Xie, D., Freire, E., and Amzel, L. M. (1994) Estimation of changes in side chain configurational entropy in binding and folding: General methods and application to helix formation, *Proteins 20*, 68−84.
25. Xie, D., and Freire, E. (1994) Molecular basis of cooperativity in protein folding. V. Thermodynamic and structural conditions for the stabilization of compact denatured states, *Proteins 19*, 291−301.
26. Murphy, K. P., Xie, D., Thompson, K. S., Amzel, L. M., and Freire, E. (1994) Entropy in biological binding processes: Estimation of translational entropy loss, *Proteins 18*, 63−67.
27. Freire, E. (1993) Structural thermodynamics: Prediction of protein stability and protein binding affinities, *Arch. Biochem. Biophys. 303*, 181−184.
28. Murphy, K. P., Xie, D., Garcia, K. C., Amzel, L. M., and Freire, E. (1993) Structural energetics of peptide recognition: Angiotensin II/antibody binding, *Proteins 15*, 113−120.
29. Murphy, K. P., Bhakuni, V., Xie, D., and Freire, E. (1992) Molecular basis of cooperativity in protein folding. III. Structural identification of cooperative folding units and folding intermediates, *J. Mol. Biol. 227*, 293−306.
30. Murphy, K. P., and Freire, E. (1992) Thermodynamics of structural stability and cooperative folding behavior in proteins, *Adv. Protein Chem. 43*, 313−361.
31. Freire, E., and Murphy, K. P. (1991) Molecular basis of cooperativity in protein folding, *J. Mol. Biol. 222*, 687−698.
32. Gómez, J., and Freire, E. (1995) Thermodynamic Mapping of the Inhibitor Site of the Aspartic Protease Endothiapepsin, *J. Mol. Biol. 252*, 337−350.
33. Murphy, K. P., Xie, D., Garcia, K. C., and Amzel, L. M. (1993) Structural energetics of peptide recognition: Angiotensin II/antibody binding, *Proteins: Struct., Funct., Genet. 15*, 113−120.
34. Ross, P., and Subramanian, S. (1982) Thermodynamics of protein association reactions: Forces contributing to stability, *Biochemistry 20*, 3096−3102.
35. Feng, S., Chen, J. K., Yu, H., Simon, J. A., and Schreiber, S. L. (1994) Two Binding Orientations for Peptides to the Src SH3 Domain: Development of a General Model for SH3-Ligand Interactions, *Science 266*, 1241−1246.
36. Booker, G. W., Gout, I., Downing, A. K., Driscoll, P. C., Boyd, J., Waterfield, M. D., and Campbell, I. D. (1993) Solution Structure and Ligand-Binding Site of the SH3 Domain of the p85α Subunit of Phosphatidylinositol 3-Kinase, *Cell 73*, 813−822.
37. Yu, H., Rosen, M. K., Shin, T. B., Seidel-Dugan, C., Brugge, J. S., and Schreiber, S. L. (1992) Solution Structure of the SH3 Domain of Src and Identification of Its Ligand-Binding Site, *Science 258*, 1665−1667.
38. Musacchio, A., Noble, M., Pauptit, R., Wierenga, R., and Saraste, M. (1992) Crystal structure of a Src-homology 3 (SH3) domain, *Nature 359*, 851−855.
39. Horita, D. A., Baldisseri, D. M., Zhang, W., Altieri, A. S., Smithgall, T. E., Gmeimer, W. H., and Byrd, R. A. (1998) Solution Structure of the Human Hck SH3 Domain and Identification of its Ligand Binding Site, *J. Mol. Biol. 278*, 253−265.
40. Hilser, V. J., and Freire, E. (1996) Structure Based Calculation of the Equilibrium Folding Pathway of Proteins. Correlation with Hydrogen Exchange Protection Factors, *J. Mol. Biol. 262*, 756−772.
41. Hilser, V. J., and Freire, E. (1997) Predicting the Equilibrium Protein Folding Pathway: Structure-Based Analysis of Staphylococcal Nuclease, *Proteins: Struct., Funct., Genet. 27*, 171−183.
42. Hilser, V. J., Townsend, B. D., and Freire, E. (1997) Structure-Based Statistical Thermodynamic Analysis of T4 Lysozyme Mutants: Structural Mapping of Cooperative Interactions, *Biophys. Chem. 64*, 69−79.
43. Hilser, V. J., Dowdy, D., Oas, T. G., and Freire, E. (1998) The Structural Distribution of Cooperative Interactions in Proteins: Analysis of the Native State Ensemble, *Proc. Natl. Acad. Sci. U.S.A. 95*, 9903−9908.
44. Cordier, F., Wang, C., Grzesiek, S., and Nicholson, L. K. (2000) Ligand-Induced Strain in Hydrogen Bonds of the c-Src SH3 Domain Detected by NMR, *J. Mol. Biol. 304*, 497−505.
45. Hamburger, J. B., Ferreon, J. C., Whitten, S. T., and Hilser, V. J. (2004) Thermodynamic Mechanism and Consequences of the Polyproline II (P_{II}) Structural Bias in the Denatured States of Proteins, *Biochemistry*, in press.
46. Creamer, T. P. (1998) Left-Handed Polyproline II Helix Formation Is (Very) Locally Driven, *Proteins: Struct., Funct., Genet. 33*, 218−226.
47. Kelly, M., Chellgren, B. W., Rucker, A. L., Troutman, J. M., Fried, M. G., Miller, A.-F., and Creamer, T. P. (2001) Host−guest study of left-handed polyproline II helix formation, *Biochemistry 40*, 14376−14383.
48. Koradi, R., Billeter, M., and Wüthrich, K. (1996) MOLMOL: A program for display and analysis of molecular structures, *J. Mol. Graphics 14*, 51−55.

BI049752M